

# Granular contact forces: proof of “self-ergodicity” by generalizing Boltzmann’s *stosszahlansatz* and *H* theorem

Philip T. Metzger\*

KSC Applied Physics Laboratory, John F. Kennedy Space Center, NASA  
YA-C3-E, Kennedy Space Center, Florida 32899

(Dated: June 2, 2006)

Ergodicity is proved for granular contact forces. To obtain this proof from first principles, this paper generalizes Boltzmann’s *stosszahlansatz* (molecular chaos) so that it maintains the necessary correlations and symmetries of granular packing ensembles. Then it formally counts granular contact force states and thereby defines the proper analog of Boltzmann’s *H* functional. This functional is used to prove that (essentially) all static granular packings must exist at maximum entropy with respect to their contact forces. Therefore, the propagation of granular contact forces through a packing is a truly ergodic process in the Boltzmannian sense, or better, it is *self-ergodic*. Self-ergodicity refers to the non-dynamic, internal relationships that exist between the layer-by-layer and column-by-column subspaces contained within the phase space locus of any particular granular packing microstate. The generalized *H* Theorem also produces a recursion equation that may be solved numerically to obtain the density of single particle states and hence the distribution of granular contact forces corresponding to the condition of self-ergodicity. The predictions of the theory are overwhelmingly validated by comparison to empirical data from discrete element modeling.

PACS numbers: 45.70.Cc, 05.20.Gg, 05.65.+b

## I. INTRODUCTION

It is interesting that the distribution of granular contact forces,  $P_f(f)$ , appears to have an asymptotically exponential tail [1–3]. In statistical mechanics, an exponential tail appears in the distribution of positive-valued variables (like particle energies) when (1) the system-wide sum of those variables is conserved, and (2) the ensemble has a flat measure. In thermal systems like a dilute, classical gas, the first of these conditions is automatically satisfied if the particle dynamics conserve energy one collision at a time. The second condition requiring a flat measure is more difficult to prove. There is an ergodic theorem based on the Poincaré cycle, which predicts the flat measure in that all accessible states will be visited with equal probability. Unfortunately this Poincaré cycle has a period greater than the age of the universe and says nothing about the measure over timescales that we observe. Boltzmann’s *H* Theorem, on the other hand, predicts the flatness in the relevant time scale, but it does so at the cost of introducing a new *a priori* assumption, albeit a very reasonable one: that colliding particles are not correlated before they collide. Therefore, the two-point correlation function describing two particles colliding is written as

$$F(\vec{p}_1, \vec{p}_2, t) = f(\vec{p}_1, t) \cdot f(\vec{p}_2, t) \quad (1)$$

where  $f$  is the single particle density of states. This is Boltzmann’s *stosszahlansatz*, or his “assumption of molecular chaos.” The subsequent proof found in his

*H*-Theorem (not repeated here) tells us that an ensemble of systems describable by Eq. 1 after following even a very tiny segment of the Poincaré cycle will have a distribution of momenta (and energies) that is the same as the average over the entire Poincaré cycle. Therefore, if Boltzmann’s *stosszahlansatz* is valid, the second condition listed above can be relaxed: we do not need a flat measure over the entire accessible region, we need only a little bit of dynamics on any part of the accessible region to obtain the necessary flatness in the practical sense.

So if this is what causes the exponential tail in a thermodynamic system, then what causes the tail in a static granular packing? As it turns out, it is caused by the same two conditions listed above. This paper shall explain the unique character of the “conservation laws” in a granular packing and how they are analogous to energy conservation in a thermal system, but with an important difference. This paper shall also explain what part of the physics causes the contact forces in a granular ensemble to spread out with a flat measure. Following Boltzmann’s lead, we do not really need to assume the measure is flat over the entire accessible part of phase space. All we need to do is write a transport equation that explains how the stress state of individual grains connects to the stress state of their neighbors, and develop an analogous version of Boltzmann’s *stosszahlansatz* and *H* Theorem.

The goal in this paper shall be to explain the ideas physically, not just mathematically, and with as much clarity as possible. To do this, Sec. II will look at several models with increasing complexity to identify the essential parts of the physics that determine the statistical mechanics of granular contact forces. After we have seen them, in Sec. III it will be a simple matter to write the equations and produce the generalized *stosszahlansatz*.

---

\*Electronic address: Philip.T.Metzger@nasa.gov

It will be asserted as a very reasonable assumption from first principles, just like Boltzmann's version, but it will also be supported by empirical observations. Sec. IV will then write the transport equation for single grain states. Assuming the generalized *stosszahlansatz* is valid, it will formally prove that essentially every accessible packing state must exist at maximum contact force entropy, and thus each packing state has the same statistical properties as an ergodic average over all states in the ensemble. This will be analogous to Boltzmann's *H* Theorem, although it will be adapted to the unique features of a granular packing. Thus, we will have achieved an ergodic proof in the Boltzmannian sense. However, it is better not to call it *ergodicity*, but rather *self-ergodicity* because a static granular packing, being *static*, does not explore phase space. The ergodicity consists of a special set of relationships that exist among the values of its phase space coordinates. The proof of this self-ergodicity stands or falls with the validity of the *stosszahlansatz*. Therefore, Sec. V will test the predictions empirically through comparison with discrete element modeling (DEM) data. The evidence overwhelmingly validates the theory. This paper leads to the immediate conclusion that (in the thermodynamic limit) every set of first shell states is equally probable in a granular packing, subject to the conservation laws. This opens the door to wider applications of statistical mechanics in granular media.

## II. THE UNIQUENESS OF GRANULAR CONTACT FORCE PHYSICS

### A. The $q$ Model: Ergodicity in One Dimension

A granular packing is static and cannot explore its phase space. So how then does the distribution of contact forces statistically relax to have an asymptotically exponential tail? The  $q$  model [4] begins answering this question. A particular example of a  $q$  model lattice is illustrated in Fig. 1, consisting of a regular lattice (diamond in this case) with grains at the nodes and grain contacts along the legs. The vertical load borne by the grains in the  $i^{\text{th}}$  layer are randomly redistributed to the grains in the  $(i+1)^{\text{st}}$  layer by means of the random  $q_j^{(i)}$  variables,  $0 \leq q_j^{(i)} \leq 1$ , which tell what fraction of the vertical load goes into the contact to the grain below it to the right, the remainder going to the grain below it to the left. After some 20 or so layers the model begins to relax so that the distribution of vertical forces has an asymptotically exponential tail. In this model, the exploration of phase space is not through the time dimension, but through a spatial dimension. All the vertical forces in one layer of the lattice form the coordinates in a single-layer phase space, and translating through the lattice layer-by-layer does explore that space.

It may be noted that the symmetry of the  $q$  model may be improved by considering the case without gravity so

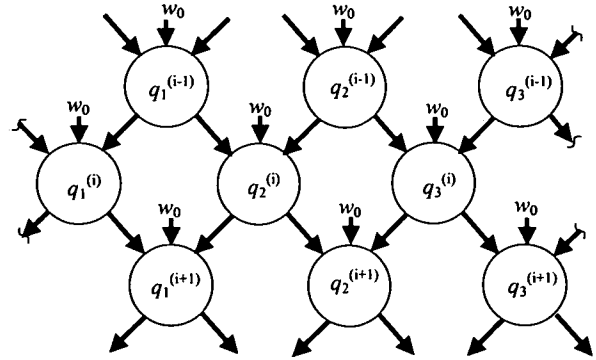


FIG. 1: A two-dimensional diamond lattice version of the  $q$  model. Forces propagate layer by layer and are redistributed in the next layer by the  $q$  values, which play the role of the collision matrix. This forms an analogy to the molecular kinetics of a gas in which the vertical dimension represents time and the complete set of molecules is a single horizontal layer.

there is no additional weight  $w_0$  applied to each grain (the injection term). Then, after a  $q$  model is developed over many layers, the upper, unrelaxed levels may be discarded, keeping only a block of deeper layers that are statistically relaxed. Then it is impossible to tell which way the information was propagated across the lattice: up or down become indistinguishable. Indeed, one can apply  $q$  values and propagate forces in one of these two directions and then when the model is relaxed extract the *apparent*  $q$  values as if the forces had been propagated in the opposite direction. Call these the  $p$  values. The author has incidentally noted that for continuous distributions of the  $q$  variable  $\eta(q)$  the distribution of the  $p$  values automatically relaxes to  $\eta(p)$ , identical to the distribution of the  $q$  values. Therefore, the weightless  $q$  model does become truly symmetric under inversion when it is relaxed in all its layers. This is analogous to a box of grains in weightlessness, squeezed on all sides by the container walls. An ensemble of such packings must be symmetric under inversion (plus parity reversal in the general, sheared case), and hence are pictured well by the relaxed, weightless  $q$  model.

Coppersmith, *et al*, showed that for the case of the uniform  $q$  model where  $\eta(q) \equiv 1$  for  $0 \leq q \leq 1$ , the exploration of the vertical forces' phase space is truly ergodic in that it visits every state with equal likelihood. On the other hand, the non-uniform  $q$  models are definitely not ergodic. Since real granular packings produce a distribution of Cartesian contact forces unlike that of the uniform  $q$  model, indicating non-uniform  $\eta(q)$ , how could we claim ergodicity for a real granular packing? The answer is that the scalar  $q$  model allows too much freedom because it does not treat the full vectorial forces, and we shall see below that in the fully vectorial lattice of a granular packing an ergodic exploration of vectorial phase space is not identical to each Cartesian component

ergodically exploring its own phase space independently. But thus far in the argument, ergodicity has not been proven for real granular packings, neither for their Cartesian components of force nor for their forces vectors. We shall say that the  $q$  model is a picture of *randomization* in a granular packing rather than ergodicity until we can prove otherwise.

### B. Analogy to Thermodynamics

Coppersmith, *et al*, introduced an analogy between the  $q$  model and the molecular kinetics of a classical dilute gas to further illuminate the nature of this layer-by-layer randomization. The analogy compares the static system of contact forces to the dynamics of a dilute classical gas: the vertical dimension of the  $q$  model's lattice is analogous to the time dimension, and a single horizontal layer in the lattice (a subspace of the entire lattice's density of states) is considered to be the entirety of the thermodynamic system at any given moment of time. The "atoms" are the contacts between grains rather than the grains themselves. The "collisions" between atoms are the grains rather than the contacts. That is, a grain is a collision of the forces that exist on its contacts. The "ingoing" contacts on the upper hemisphere of the grain each carry a vertical force, which is analogous to an atom's kinetic energy, and the collision within the grain redistributes these quanta into the "outgoing" contacts on the lower hemisphere. Thus, the set of all atoms in one layer of the  $q$  model represents the same set of atoms in the next layer, after they have emerged from their collisions. An  $N \times N$  lattice represents only  $N$  atoms, not  $N^2$ . In summary, one spatial dimension becomes analogous to time while the other(s) represent the extent of the system at any one moment, so the set of just  $N$  atoms (contacts) within that instantaneous extent are propagated across the lattice in the remaining "time" direction. This analogy can also be extended beyond the regular lattice of the  $q$  model to the arbitrarily disordered "lattice" of a real granular packing as illustrated in Fig. 2 if we relax the constraint that particle count is conserved during the collisions.

This picture by Coppersmith, *et al*, is the beginning of a second analogy to thermodynamics that is complementary to the one put forward by Edwards [5, 6]. In the thermodynamic analogy of Edwards, the geometry of the packing is made to explore its configuration space through a series of mechanical taps, and under certain conditions it eventually relaxes to the most entropic volume, the one represented by the highest number of microstates. Thus, the Edwards ergodicity is extrinsic and dynamic, affecting the contact geometry of the packing as well as its forces. The type of randomization that is pictured by the  $q$  model is intrinsic and static, affecting only the forces which propagate through the fabric, but achieving thermalization whether or not the contact geometry has been allowed to relax. The problem with this

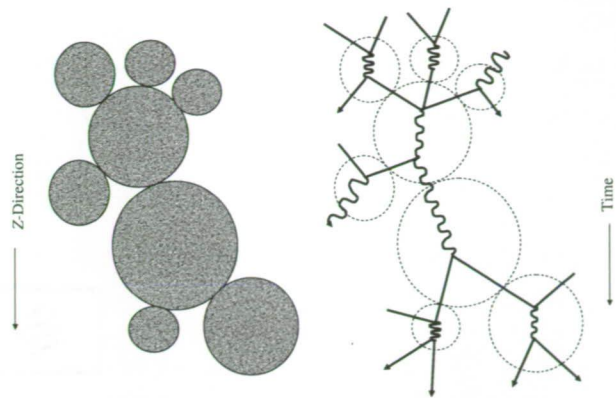


FIG. 2: Illustration of the analogy by Coppersmith, *et al*. [4], between the static granular media and thermodynamics, in which the vertical dimension is analogous to the time dimension.

new analogy, however, is that it treats only one of the spatial dimensions as analogous to the time dimension, and thus it breaks the inherent symmetries of granular ensembles. Recovering that symmetry is what leads to the full, self-ergodic theory.

### C. Ergodicity in Orthogonal Dimensions

The  $q$  model only deals with the vertical component of force ( $f_z$ ), conserving its sum layer-by-layer in the version of the  $q$  model without gravity, and illustrating a type of randomization (or ergodicity) in one conjugate spatial dimension. However, in a granular packing without gravity, the sum of the forces perpendicular to the  $x$  axis and to the  $y$  axis are also conserved layer-by-layer or column-by-column. To explain this statement and make it rigorous we must first define a "layer" of grain contacts. Referring to Fig. (3), we: (1) draw a cross-sectional line (like any one of the dashed lines in the figure), (2) select the set of grains intersected by that one line (shaded grains), and (3) include only those contacts on that set of grains (heavy dots) that (a) connect to other grains *external* to the shaded set and (b) are located *on one side* of the shaded set. Next, we decompose the forces on that set of contacts into Cartesian components parallel and normal to the dashed line. Summing all the components in the normal direction produces the "total Cartesian load" in that plane. In the absence of gravity, the total Cartesian load is conserved with respect to translation of the dashed line, as illustrated in the figure by the parallel layer of shaded grains and heavy dots. If that were not so, then the grains between the two shaded layers would be accelerating.

Generalizing the key insight of the  $q$  model, a granular packing should therefore have internal force relationships between the subspaces that represent not just the layer-by-layer subspaces in the  $z$  direction, but also the



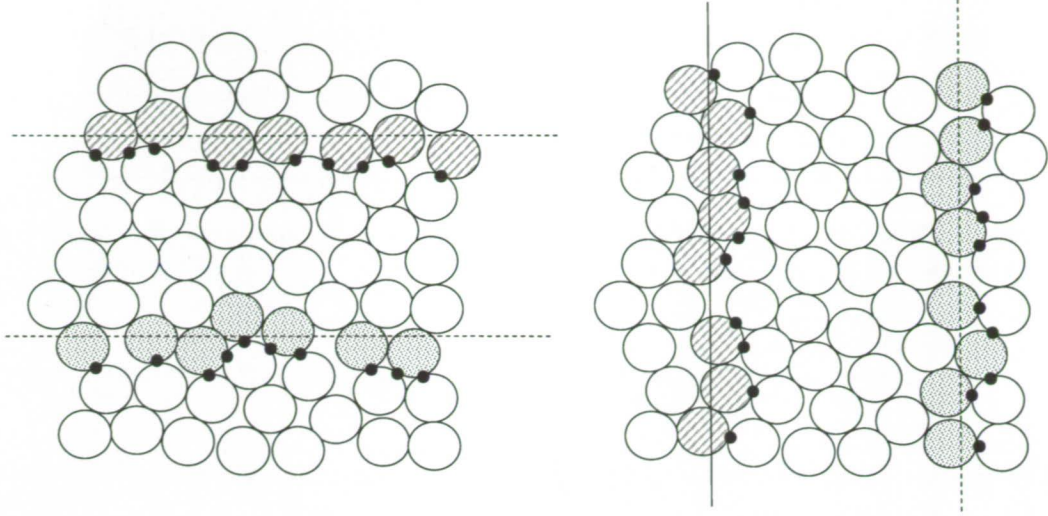


FIG. 3: Illustration how the kinetic analogy of Coppersmith, et al. [4], with respect to the  $q$  model, may be adapted to 2D granular packings.

column-by-column subspaces in the  $x$  direction and again in the  $y$  direction (for 3D packings). Each such set of relationships imply their own randomization in the corresponding direction subject to their own conservation law.

There are no equivalent subspace relationships in a classical thermal system. In an ideal gas, for example, it is extremely unlikely that the sum of the particle momenta or energies in a cross-sectional layer of the container would be the same as in any other parallel cross-sectional layer at any one moment of time. Furthermore, dynamics cause the gas to evolve ergodically so that it visits every possible state equally without regard for any subspace correlations. This is obviously not the case for static granular packings, where the relationships between neighboring layer-wise subspaces *must* exist merely because the packing is static. These internal relationships between the subspaces add a significantly new set of constraints onto the form of the overall density of states.

The thermodynamic analogy to the  $q$  model identifies the spatial dimension perpendicular to the layer as the time dimension. To extend the  $q$  model analogy to the full set of Cartesian components in a 2D granular packing, we may consider *both* spatial dimensions to be time dimensions (a “plane” of time), and *both* independently-conserved quantities (total Cartesian loads) to be energies. In 3D systems, we have three “time” dimensions and three independently conserved “energies”. These two (three) conservation laws are orthogonal to each other, so that we do not have a simple uni-directional ergodicity in the time dimension as in thermodynamics. Instead, we have two (three) randomizations (or ergodicities) that are orthogonal to one another.

#### D. Exploring Phase Space Without Moving

The key insight of the  $q$  model is that contact forces can explore phase space in a granular packing that is completely static: the exploration of phase space is not performed by the entire system as a whole through the time dimension; rather it is performed layer-by-layer in the spatial dimensions because of the static equilibrium relationships that exist between the layers.

To emphasize how unusual this concept actually is, we consider a granular packing’s phase space dynamics, or rather its lack of phase space dynamics. Each granular packing is plotted in phase space as a single point, and it remains perfectly immobile wherever it may be. We can see that there is no exploration of phase space at all. However, only certain, very special locations in phase space are valid for static granular packings. These locations have a special property in that the subspaces of the coordinates (corresponding to the individual layers of the packing) have static equilibrium relationships with one another. These relationships are such that each successive subspace has a locus that moves relative to the previous subspace according to the micromechanics of the layer of grains between them. These micromechanics conserve the sum of the subspace coordinates in each layer while also introducing a randomization from one layer to the next. Thus, there is a random walk built right into every valid locus of phase space. It is not moving in time, but it really is exploring phase space, nonetheless. Before a packing can become static it must first locate and settle upon one of these special loci that has the equivalence of motion built into itself, and not just in one dimension, but in two (or three) orthogonal decompositions simultaneously. We shall further show below that



this orthogonal, ingenerate exploration of phase space is not just randomized, but really ergodic in the Boltzmannian sense. This new type of ergodicity is a very important concept to understanding granular media and so it deserves a name. "Self-ergodicity" seems appropriate.

### E. Vectorized $q$ Model

Because these orthogonal randomizations (or self-ergodicity) appear to be the essential concept in solving granular contact force physics, it would seem important to create a version of the  $q$  model that treats the orthogonal directions correctly. However, generalizing the  $q$  model to include horizontal forces presented an interesting challenge. In one example [7], the  $q$  model was vectorized so that the full vectorial forces are propagated layer-by-layer in one direction across the lattice from top to bottom, just as in the scalar  $q$  model. As the information is propagated, vectorial force balance is enforced on each grain. This conserves the sum of the vertical forces in each layer, but the horizontal forces grow without bounds as the information progresses through the lattice. This is partly because of the direction that the horizontal forces were being propagated across the lattice. The sum of the horizontal forces in a single column cannot be enforced unless the entire column is propagated column-by-column in the horizontal direction. Propagating in that direction should allow the forces to explore phase space both up and down the column without bias, and this will statistically distribute them without bias in the upper versus lower parts of the lattice. This will solve the problem of monotonic growth from top to bottom. Stated in its essence, granular ensembles in nature are fundamentally organized to conserve horizontal forces in the horizontal direction, and so to be fundamentally meaningful a model should also be organized this way.

### F. Overlaid $q$ Models

This observation indicates another way to attempt generalizing the  $q$  model, illustrated in Fig. 4. For a 2D granular packing, we may simply implement two separate  $q$  models independently, throw away the upper, unrelaxed layers while keeping enough relaxed layers of each  $q$  model so that their lattices are square, and then rotate one of them by  $\pi/2$  radians with respect to the other. The two square lattices can then be sandwiched together so that each leg of the lattice is provided with two scalar forces, one the vertical component of force from the first  $q$  model, and the other the horizontal component of force from the rotated  $q$  model. This successfully achieves vectorial force balance on each grain and it also organizes the global conservation laws properly in each orthogonal direction so that neither component of force grows without bounds. Thus, it solves the problem of the vectorial  $q$  model described above.

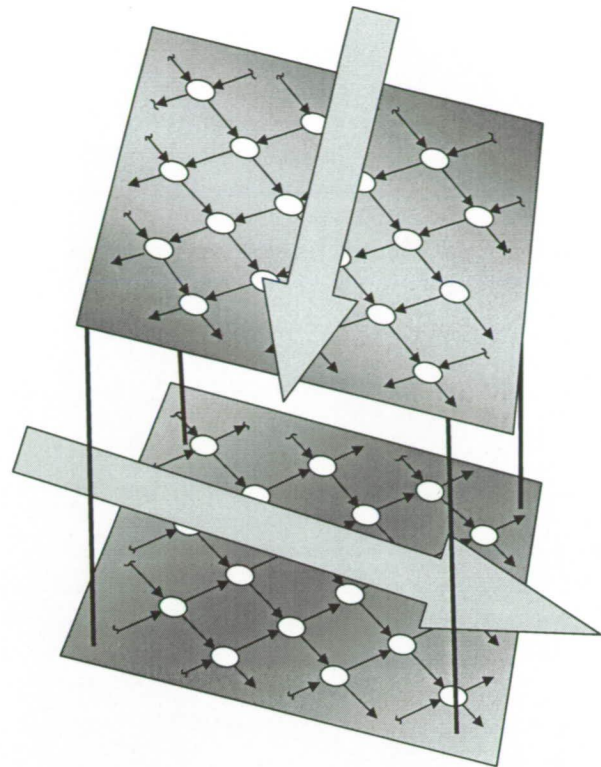


FIG. 4: Two square, relaxed sections of  $q$  models may be overlaid to produce force vectors that (1) sum to zero on every grain, and (2) properly conserve the total force in each conjugate direction. However, the correlations between force vector angles and contact surface angles are not properly organized in this model as illustrated in Fig. 5.

Unfortunately, that is not the end of the story. The resulting set of contact force vectors produced by this method is so wrong that it cannot even be considered a model of granular materials. In a real granular material, the directions of contact force vectors are correlated to the normal vectors at the contacting surfaces as illustrated in Fig. 5. For frictionless, cohesionless grains, the forces must lie perfectly on the contact normals. For Coulomb friction, the allowable force vector directions widen to become cones centered on the contact normals. For perfect friction but still no cohesion, the cones open further to become entire hemispheres looking inwardly toward the grain. For imperfect cohesion and perfect friction, the allowable directions become fully spherical for weak forces but still hemispheric for strong forces that exceed the allowable cohesion. Only in the case of perfect cohesion and perfect friction do the allowable directions of the contact force vectors become completely uncorrelated to the contact normal directions, but that is precisely the case where it is no longer a granular material. In general, the less fragile the packing, the less correlated the contact force directions are with the contact angles.



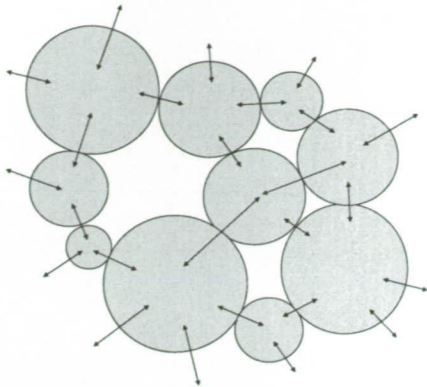


FIG. 5: In a realistic granular packing, the directions of contact force vectors cannot be random, but must be correlated to the contact surface normal directions.

Fragility is what makes a granular material essentially granular [8]. In this overlaid  $q$  model the horizontal and vertical components of force are not correlated with each other to point in any special directions, and so the resulting network of forces cannot be interpreted in any meaningful way as a granular contact geometry. In fact, solving for grain diameters on the basis of this set of force vectors and assuming no cohesion, some of the grains are found to have negative diameters, clearly demonstrating that it is not geometrically meaningful. This method also produces the incorrect form for  $P_f(f)$ , beginning from  $P_f(0) = 0$  rather than  $P_f(0) > 0$  as seen in the numerical simulations. This, too, is due to the unnatural statistical independence of the two force components at each contact.

### G. Competing Constraints in a Granular Packing

Here is an indispensable insight. The key problem in generalizing kinetic theory to contact forces inside static granular materials is that the ergodicities are orthogonal but not independent. The orthogonal conservation laws require that the components of force information propagate in their own corresponding spatial directions, but both components of force must arrive at each grain simultaneously in order to effect proper correlations between them at the contact angle. These two constraints are severe. Nature meets them, of course, by exploring the phase space through the real time dimension, in which the geometry of the grains' packing adjusts itself until it finds one of the very rare stable states in force and geometry space that meet all orthogonal conservation laws in every layer and column and all the force vector direction constraints at every grain contact.

Similarly, several lattice-based models have been devised to use the equivalence of temporal exploration of the phase space to find valid states. These models use either an iteration process on the lattice [9], or a global

annealing process that leverages hyperstaticity [10], or an iteration that is localized to the first coordination shells by leveraging hyperstaticity [11]. Following specific iterations of a model in that way is analogous to following the state of a thermodynamic system through time, which is the idea in kinetic theory. The intention of this paper, on the other hand, is to derive a solvable Boltzmann-like equation and thus to obtain a statistical mechanics theory, not a kinetic theory. Therefore, it is essential to keep the specific iterations of the actual time dimension out of this theory.

To develop a lattice model that avoids temporal iterations, we would need to propagate the waves of information in each orthogonal direction (for the conservation laws), and yet have each wave arrive at every grain in the packing simultaneously (to effect the force component correlations at the contacts). Of course, this is geometrically impossible; only a set of grains running diagonally across the lattice can receive both waves simultaneously. Therefore, we can conclude that it is impossible to generalize a  $q$  model in a way that is organized fundamentally the same as nature's granular packings (without resorting to nature's temporal iterations). The solution to this problem is to dispense with the lattice. We must collapse the density of multi particle states to a density of single particle states. That way, we can propagate the information to every particle in the density of states simultaneously while enforcing all of the conservation laws. Instead of following Liouville or Gibbs with multi-particle phase spaces, we shall follow Boltzmann with single particle distributions. This Boltzmannian approach allows us to "collide" grains together without knowledge of their spatial arrangement in the lattice. However, without any knowledge of the spatial arrangement, we will need the equivalent of Boltzmann's *stosszahlansatz* to tell us how to deal with any spatial correlations that may exist. Since granular packings have the analog of multiple "time" dimensions, this *stosszahlansatz* must be generalized in a way that properly maintains the extra symmetries of the physics.

### III. THE GENERALIZED STOSSZAHLANSATZ

It will be shown below that the properly symmetric version of the *stosszahlansatz* is obtained automatically by taking the First Shell Approximation in the fabric in the density of multi particle states before collapsing it to a density of single particle states. We will take four steps to develop this idea. First, the density of multi particle states will be described from first principles as our starting point. Second, to understand how we must modify this density of states, qualitative arguments will be provided to show that the First Shell Approximation does not discard essential force correlations in the packing, just as Boltzmann's *stosszahlansatz* does not discard essential momentum correlations in the state of a dilute gas. In thermodynamics, Boltzmann's *stosszahlansatz*

seems eminently reasonable, but a rigorous proof is lacking and so empirical testing is required. Likewise, the qualitative arguments provided here indicate that the First Shell Approximation is reasonable, but in the end testing will be required. Third, we will mathematically analyze the First Shell Approximation and finish with an expression that is recognizable by its form as the generalized version of Boltzmann's *stosszahlansatz*. This will demonstrate that the First Shell Approximation really does perform the same function for self-ergodicity as Boltzmann's assumption does for thermal ergodicity. Fourth, just as Boltzmann's assumption in thermal systems required empirical validation, so empirical validation will be required for the generalized version. These shall be kept to the end of the paper after the theory's predictions are fully developed. These results shall indicate that the generalized *stosszahlansatz* is excellent, perhaps to the same degree of rigor if not better than Boltzmann's original version in thermal systems.

### A. The Density of Multi Particle States

The microcanonical density of multi particle states has been written [12–14] for static granular packings of rigid, round, frictionless grains (without the symmetry-breaking effect of gravity) in the form,

$$\begin{aligned} \rho\{\text{forces, geometry}\} = & \prod_{\text{contacts}} \delta(\text{Newton's Third Law}) \\ & \times \Theta(\text{No Overlapping Grains}) \\ & \times \prod_{\text{grains}} \delta(\text{Newton's Second Law}) \\ & \times \prod_{\text{contacts}} \Theta(\text{No Tensile Forces}) \\ & \times \delta(\text{Specified Stress State}) \\ & \times \delta(\text{Specified Fabric State}). \quad (2) \end{aligned}$$

with the expressions,

$$\begin{aligned} \rho\{f^{\mu\nu}, \zeta \mid \mathcal{C}\} = & \mathcal{N} \left\{ \prod_{(\alpha\gamma, \beta\delta) \in \mathcal{C}} \delta(\vec{f}^{\alpha\gamma} - \vec{f}^{\beta\delta}) \right\} \Theta_{\zeta}(\zeta \mid \mathcal{C}) \\ & \times \left\{ \prod_{\alpha=1}^N \delta\left(\sum_{\gamma=1}^{Z^{\alpha}} \vec{f}^{\alpha\gamma}\right) \prod_{\gamma=1}^{Z^{\alpha}} \Theta(f^{\alpha\gamma}) \right\} \\ & \times \prod_{i,j=x,y} \delta\left(\sum_{\alpha,\beta} f_i^{\alpha\beta} l_j^{\alpha\beta} - D_{ij}\right) \\ & \times \delta(P_{4\theta} - Q_{4\theta}(\zeta)). \quad (3) \end{aligned}$$

It was adapted from Edwards' microcanonical density of states in the geometric information [5] and from Edwards' and Grinev's stress probability functional in the force information [15]. It assumes Edwards' flat measure in the geometry and isostacy in the forces. Packings in the perfectly frictionless, perfectly rigid idealization do appear

to be isostatic in numerical simulations [16]. In this equation, the geometrical information of the packing is contained in the set of variables  $\zeta$ . The contact force on grain  $\mu$  on its contact  $\nu$  is  $f^{\mu\nu}$ . The construction list  $\mathcal{C}$  tells which  $(\mu\nu) = (\alpha\gamma)$  connects to  $(\mu\nu) = (\beta\delta)$ , and hence is a part of the geometric information otherwise included in  $\zeta$ .  $\mathcal{C}$  is written explicitly because it will be important to the derivations later in this paper. The function  $Q_{4\theta}$  computes the generalized fabric of the packing,  $P_{4\theta}(\theta_1, \theta_2, \theta_3, \theta_4)$  [17]. Although this  $P_{4\theta}$  nomenclature implies that every grain has exactly  $Z = 4$  contacts,  $P_{4\theta}$  may be understood more generally as a statistical summary of all the contact angle information of the grains within their first coordination shells, regardless of their  $Z$ . The function  $\Theta_{\zeta}$ , introduced by Edwards [5], enforces non-overlapping of the grains such that each packing is physically realizable. Here,  $\Theta_{\zeta}$  serves this purpose only in the second and higher coordination shells, since  $P_{4\theta}$  is sufficient to perform that same function within the first coordination shell.

The *duress* tensor  $D_{ij}$  is defined as the extensive counterpart to the stress tensor,

$$\begin{aligned} D_{ij} = & (\text{Area}) \times \sigma_{ij} \quad (\text{for 2D packings}) \\ = & (\text{Volume}) \times \sigma_{ij} \quad (\text{for 3D packings}). \quad (4) \end{aligned}$$

That is, it is a rank two tensor that has the units of force  $\times$  distance and represents the total of all forces operating across their branch vector lengths within the volume of the packing. In the thermodynamic analogy, all the spatial dimensions are like time dimensions and so the multi-dimensional "duration" of the stress in a region of grains is the volume of that region. Hence, duration multiplied by stress is duress, which explains the name. It is related to the strain energy of an elastic system, although in a perfectly rigid granular packing there is no elastic strain energy.

As explained in [12], it is possible in the idealized  $Z = 4$  case to change the coordinates of  $\rho$  from  $(\vec{f}^{\mu\nu}, \zeta)$  to  $(w_x^{\mu}, w_y^{\mu}, \zeta)$  where the Cartesian loads are defined as

$$w_x^{\mu} = \frac{1}{2} \sum_{\nu=1}^{Z^{\mu}} f^{\mu\nu} |\cos \theta^{\mu\nu}|, \quad w_y^{\mu} = \frac{1}{2} \sum_{\nu=1}^{Z^{\mu}} f^{\mu\nu} |\sin \theta^{\mu\nu}|. \quad (5)$$

In the  $Z = 4$  case, specifying  $(w_x, w_y, \theta_1, \dots, \theta_4)$  permits all four contact forces to be solved trigonometrically,  $\vec{f}_{\eta} = \vec{f}_{\eta}(g)$  for  $\eta = 1, 2, 3$ , and 4. For  $Z \neq 4$  either more or fewer state variables should be specified.

### B. Qualitative Arguments for the First Shell Approximation

Eq. 3 specifies the generalized fabric  $P_{4\theta}$  as part of the definition of the microcanonical ensemble. This function imposes steric exclusion in the first coordination shell, because it evaluates to zero whenever  $\theta_i$  and  $\theta_j$  ( $i \neq j$ )



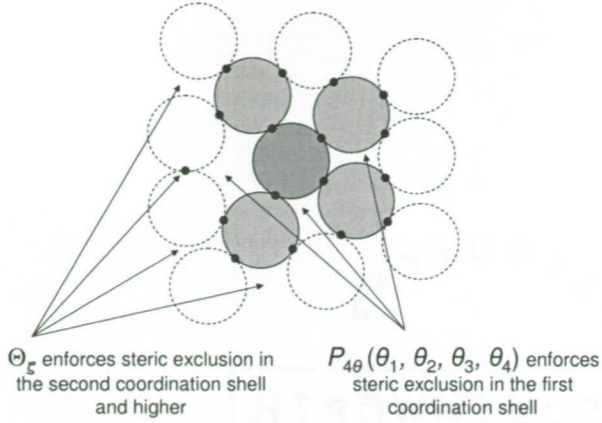


FIG. 6: Illustration of coordination shells. The central grain is shaded dark. The first coordination shell is shaded lightly. The second coordination shell is dashed and unshaded. Simply omitting  $\Theta_\zeta$  from the density of states is the First Shell Approximation.

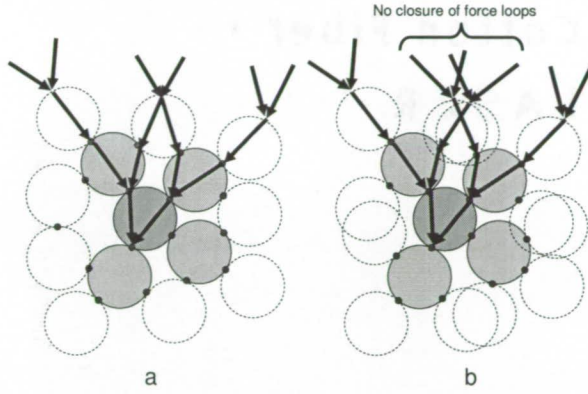


FIG. 7: (Left) When  $\Theta_\zeta$  is kept as part of the density of states, forces form loops and so "colliding" forces on the central grain may have pre-correlation, because they have seen parts of each other before. (Right) When  $\Theta_\zeta$  is omitted from the density of states, which is the First Shell Approximation, then force loops do not close and so colliding forces are not pre-correlated by the packing. The only correlation arises from the stability requirements of the central grain, itself.

are within  $\pi/3$  of one another (as an example for the case of monodisperse spheres). The purpose of  $\Theta_\zeta$  is to enforce steric exclusion in the second and higher coordination shells, as illustrated in Fig. 6. Thus, eliminating  $\Theta_\zeta$  from Eq. 3 is the First Shell Approximation, keeping steric exclusion in the first coordination shell via  $P_{4\theta}$  but ignoring all geometric constraints in the shells further away. Fig. 7 shows that eliminating  $\Theta_\zeta$  assures that the packings having closed force loops outside the first coordination shell will comprise a set of zero measure, not affecting the statistics of the ensemble. Therefore, we may say that (essentially) all forces arriving at a grain will

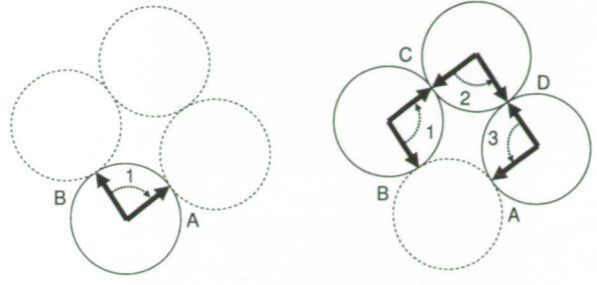


FIG. 8: Correlations between neighboring contact forces may arise two different ways. (Left) They arise through intra-grain stability requirements, resulting in a strong, two-point correlation between the forces at  $B$  and  $A$ . (Right) They arise through a series of intra-grain stability requirements working grain-by-grain around the loops, resulting in weak higher-order correlations. The example here shows a four-point correlation through the loop,  $B$  to  $C$  to  $D$  to  $A$ , which will be much weaker than the two-point correlation directly from  $B$  to  $A$ .

have arrived directly from infinity without ever interacting with one another. Thus it ensures that no correlation between colliding forces can arise in the packing, apart from the stability requirements of the central grain itself. In the First Shell Approximation, all correlation is intra-grain and propagates outward through the packing; no correlation arises non-locally in the lattice propagating inward to shape the statistics of the central grain. This explains how the First Shell Approximation is equivalent to the generalized Boltzmann assumption.

Fig. 8 shows that the correlations due to those force loops are negligible and hence can be reasonably discarded. Correlations between neighboring contacts on the same grain arise either through the grain itself or through the loops in the packing. A typical loop is four or more grains, so going the long way around a loop induces a weak third-order correlation, but going the short way between the two contacts (staying intra-grain) induces a very strong first-order correlation. The First Shell Approximation discards the very weak four point correlation but keeps the very strong two-point correlation. Thus, it is equivalent to truncating the BBGKY hierarchy, which in thermal statistical mechanics is equivalent in effect to Boltzmann's *stosszahlansatz*.

It has been shown [2] that contact forces on the same grain are strongly correlated with one another. There is anti-correlation for contacts closer together than roughly  $\pi/2$  radians of angular separation, and positive correlation when the angular separation is greater than roughly  $\pi/2$ . The correlation continues to increase as the contacts are increasingly distant from one another but still on the same grain. These strong intra-grain relationships make sense due to the requirements of static equilibrium of the individual grains. Contacts on the same quadrant compete for a share of the same load and hence are anti-correlated. Contacts opposite one another transmit load



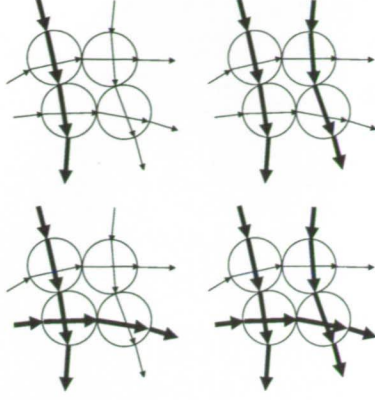


FIG. 9: Contacts that are approximately  $\pi/2$  radians away from one another on the same grain are only weakly correlated as illustrated by the closed loop of four grains that allows any combination of weak and strong force chains to pass through it. If the angles were precisely  $\pi/2$ , then the four force chains in this figure would be completely independent.

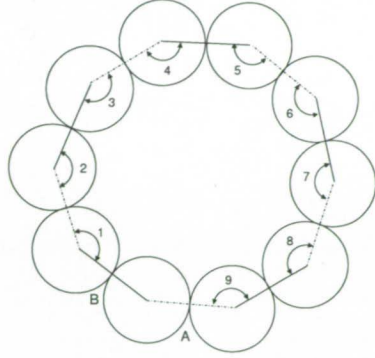


FIG. 10: Contacts that are highly correlated are close to  $\pi$  radians apart on the same grain [2]. Hence, a closed loop composed of highly correlated pairs of contacts can turn only very slowly and must pass through a very large number of grains.

through one another and hence are correlated. Simplistically we could expect  $\pi/2$  to be the crossover point of no correlation as illustrated in Fig. (9). This is important, because small loops of grains are formed through adjacent pairs of contacts that are closer to  $\pi/2$  than  $\pi$  radians of separation, and hence there is minimal correlation in each two-point leg of a force loop. The net four point correlation, which we have already argued to be weak, is therefore even weaker than what we would expect in a thermal system. On the other hand, force loops that pass through grains with closer to  $\pi$  radians of separation will require a vastly larger number of grains in the loop to slowly turn through the full  $2\pi$  radians to close the loop as illustrated in Fig. 10, and these  $N$ -point correlations ( $N \gg 4$ ) will be extraordinarily weak.

The total correlation between a pair of contacts on a

grain must be the sum of information from *all* the loops in the packing that contain the grain in question. Due to the disorder of the packing and the large number of loops that contain the same grain, some correlating and some anti-correlating, it is expected that the contributions from increasingly larger loops of grains will be increasingly decoherent and largely cancel one another.

From these arguments there is good reason to assume *a priori* that the intra-grain contribution to the correlations is the dominant one. Thus, it appears reasonable that the first shell approximation does not discard essential correlations from a granular packing.

### C. Mathematical Derivation from the First Shell Approximation

These physical arguments are the basic idea behind using the first shell approximation as the *stosszahlansatz*, and now this idea shall be developed mathematically. The first step in collapsing the multi-particle density of states to a single particle density of states is to sum  $\rho$  over all grain exchanges represented by the  $N!$  possible construction lists  $C_k$ ,

$$\tilde{\rho}\{f^{\mu\nu}, \zeta \mid P_{4\theta}, D_{ij}\} = \mathcal{N} \sum_{k=1}^{N!} \rho\{f^{\mu\nu}, \zeta \mid C_k, P_{4\theta}, D_{ij}\} \quad (6)$$

where the tilde on  $\rho$  indicates that this density is in an *assembly space* rather than a phase space. Each locus in an assembly space specifies a set of single grain configurations, and the density in this space tells how many valid packing states may be *assembled* by connecting together the grains from that set. All terms in Eq. 3 factor out from the sum except  $\Theta_\zeta$  and the product over the delta functions enforcing Newton's Third Law,

$$\begin{aligned} \tilde{\rho}\{f^{\mu\nu}, \zeta \mid P_{4\theta}, D_{ij}\} &= \left\{ \sum_{k=1}^{N!} \Theta_\zeta(\zeta \mid C_k) \prod_{C_k} \delta^2(\vec{f}^{\alpha\gamma} + \vec{f}^{\beta\delta}) \right\} \\ &\times \left\{ \prod_{\alpha=1}^N \delta \left( \sum_{\gamma=1}^{Z^\alpha} \vec{f}^{\alpha\gamma} \right) \prod_{\gamma=1}^{Z^\alpha} \Theta(f^{\alpha\gamma}) \right\} \\ &\times \prod_{i,j=x,y} \delta \left( \sum_{\alpha,\beta} f_i^{\alpha\beta} l_j^{\alpha\beta} - D_{ij} \right) \\ &\times \delta(P_{4\theta} - Q_{4\theta}(\zeta)). \end{aligned} \quad (7)$$

We call the summation in the brackets  $\Phi$ ,

$$\Phi = \sum_{k=1}^{N!} \Theta_\zeta(\zeta \mid C_k) \prod_{C_k} \delta^2(\vec{f}^{\alpha\gamma} + \vec{f}^{\beta\delta}) \quad (8)$$

We wish to determine the behavior of  $\Phi$  in the thermodynamic limit (very large  $N$ ). Unless we discard  $\Theta_\zeta$  we can make no progress. All of the subsequent development results from this First Shell Approximation. We

may expand the product over  $C_k$ ,

$$\Phi = \lim_{N \rightarrow \infty} \sum_{k=1}^{N!} \prod_{\alpha=1}^N \prod_{\gamma=1}^4 \prod_{\beta=\alpha}^N \prod_{\delta=1}^4 \delta_{C_k} \delta^2(\tilde{f}^{\alpha\gamma} - f^{\beta\delta}) \quad (9)$$

where the Kronecker delta function  $\delta_{C_k}$  is nonzero only for contact pairs contained within list  $C_k$ . Note that the product in  $\beta$  is only from  $\alpha$  to  $N$ , the upper triangle in the  $(\alpha, \beta)$  plane. This prevents enforcement of Newton's Third Law twice for every contact, once looking from grain  $\alpha$  to grain  $\beta$  and again from  $\beta$  to  $\alpha$ , and produces the correct number of delta functions so that the units of  $\bar{\rho}$  are correct. However, we actually want the symmetry of looking both ways since the ensemble is symmetric with respect to rotating the granular packings by  $\pi$  radians, and so in the next step we sum over the entire  $(\alpha, \beta)$  plane, doubling the number of delta functions, and we must write it as  $\Phi^2$ ,

$$\Phi^2 = \lim_{N \rightarrow \infty} \sum_{k=1}^{N!} \prod_{\alpha=1}^N \prod_{\gamma=1}^4 \prod_{\beta=1}^N \prod_{\delta=1}^4 \delta_{C_k} \delta^2(\tilde{f}^{\alpha\gamma} - \tilde{f}^{\beta\delta}). \quad (10)$$

Next we commute the sum in  $k$  inside the two products.

$$\begin{aligned} \Phi^2 &= \lim_{N \rightarrow \infty} \mathcal{M} \prod_{\alpha=1}^N \prod_{\gamma=1}^4 \sum_{k=1}^{N!} \prod_{\beta=1}^N \prod_{\delta=1}^4 \delta_{C_k} \delta^2(\tilde{f}^{\alpha\gamma} - \tilde{f}^{\beta\delta}) \\ &= \lim_{N \rightarrow \infty} \mathcal{M} \prod_{\alpha=1}^N \prod_{\gamma=1}^4 \sum_{\beta=1}^N \sum_{\delta=1}^4 \delta^2(\tilde{f}^{\alpha\gamma} - \tilde{f}^{\beta\delta}) \end{aligned}$$

This introduces a need for renormalization with  $\mathcal{M}$  because each of the terms in the product is now a sum of many delta functions instead of just one delta function, vastly increasing the number of states in  $\rho$ . However,  $\mathcal{M}$  will be suppressed henceforth since the normalization has no effect on the derivation. This commutation also introduces an error because the product of all these sums expands to a sum of the product of all possible combinations of the delta functions with replacement, whereas it should have been without replacement. In the limit  $N \rightarrow \infty$  this error vanishes, because the majority of the terms in the product of delta functions will have the same representative distribution of grains  $\rho_g$ , whereas the cross-terms with significantly deviating  $\rho_g + \Delta\rho_g$  will be a vanishingly small fraction and make zero contribution to the sum in that limit. Therefore, the renormalization of the increased number of states is trivial.

Next, we expand the delta functions as the difference between two step functions with the limit of vanishing distance between them and with magnitudes proportional to the inverse of that distance.

$$\begin{aligned} \Phi^2 &= \lim_{N \rightarrow \infty} \prod_{\alpha=1}^N \prod_{\gamma=1}^4 \sum_{\beta=1}^N \sum_{\delta=1}^4 \lim_{\Delta f \rightarrow 0} \frac{1}{\Delta f} \lim_{\Delta \theta \rightarrow 0} \frac{1}{\Delta \theta} \\ &\times \{ \Theta[f^{\beta\delta} - f_i(f^{\alpha\gamma})] - \Theta[f^{\beta\delta} - f_{i+1}(f^{\alpha\gamma})] \} \\ &\times \{ \Theta[|\theta^{\beta\delta} - \theta_j(\theta^{\alpha\gamma})| - \pi] \\ &\quad - \Theta[|\theta^{\beta\delta} - \theta_{j+1}(\theta^{\alpha\gamma})| - \pi] \} \quad (11) \end{aligned}$$

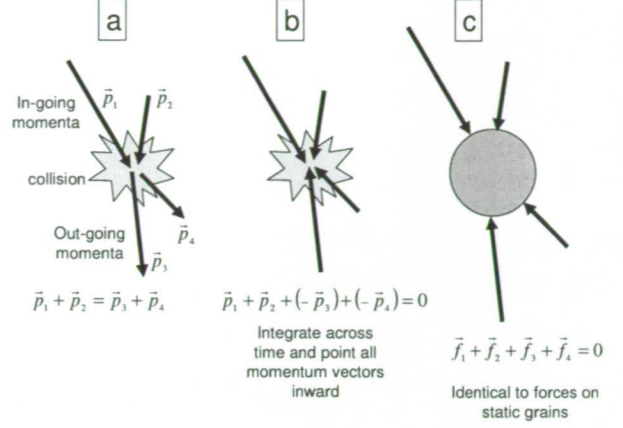


FIG. 11: Illustration how momentum vectors in binary collisions of a dilute gas are analogous to contact forces on a static grain. Boltzmann wrote the *stosszahlansatz* with preference for the in-going momentum vectors, but for static granular materials the symmetries among the contact force vectors must be restored.

where the subscripts  $i$  and  $j$  define the  $i^{\text{th}}$  interval of the force axis as the interval containing  $f^{\alpha\gamma}$  and the  $j^{\text{th}}$  interval of the angle axis as the interval containing  $\theta^{\alpha\gamma}$ . Taking the summations,

$$\Phi^2 = \lim_{N \rightarrow \infty} \lim_{\Delta f \rightarrow 0} \lim_{\Delta \theta \rightarrow 0} \frac{1}{\Delta f} \frac{1}{\Delta \theta} \prod_{\alpha=1}^N \prod_{\gamma=1}^4 n_{ij} \quad (12)$$

where  $n_{ij}$  is the number of grains in the summation that fall into the space between the step functions in the  $i^{\text{th}}$  bin of the force axis and the  $j^{\text{th}}$  bin of the angle axis. Taking the limits converts  $n_{ij} \rightarrow P_{f\theta}$ , and taking the square root of both sides recovers  $\Phi$  in a usable form,

$$\Phi = \prod_{\alpha=1}^N \Upsilon_{\alpha} \quad (13)$$

where

$$\Upsilon_{\alpha} = \prod_{\gamma=1}^4 P_{f\theta}^{1/2}(f^{\alpha\gamma}, \theta^{\alpha\gamma}) \quad (14)$$

or, simplifying notation,

$$\Upsilon_{\alpha} = \prod_{\gamma=1}^4 P_{f\theta}^{1/2}(\tilde{f}^{\alpha\gamma}) \quad (15)$$

Now we are in a position to see that this is the properly symmetric generalization of Boltzmann's *stosszahlansatz*. Referring to Fig. 11, in a particle collision the sum of the momentum vectors is conserved. Hence, if the outgoing momentum vectors are reversed, then the sum of all four momentum vectors will equal precisely zero. Putting a little space between the four vectors and drawing a circle,



we see that this set of four vectors is identical to four contact forces on a static grain. However, Boltzmann wrote the *stosszahlansatz* with preference for the forward time direction, and therefore he wrote that only the incoming pair of vectors are statistically uncorrelated.

$$F(\vec{p}_1, \vec{p}_2, t) = f(\vec{p}_1, t) \cdot f(\vec{p}_2, t) \quad (16)$$

If we try to apply this to granular contact forces, we could group the four forces on the grain into six different pairs, and there is no reason why one of those pairs should be written as uncorrelated to the exclusion of the other five. Comparing Eq. 15 to Eq. 16, we see that the former is a product over all four vectors, preserving the symmetry. Furthermore, the  $1/2$  power represents the analog of time-reversal symmetry. This is because the product in  $\alpha$  includes all grains, so that a grain and its contacting neighbor are both included somewhere in the product. Thus,  $1/2$  power of a term is included with grain  $\alpha$ , whereas the other  $1/2$  power of the same term is included with the contacting grain where the same force vector is looking in the opposite direction (time reversal symmetry). Thus, the generalized version of the *stosszahlansatz* not only treats all force vectors on a grain symmetrically, it also maintains the symmetry of Newton's third law between grains.

For comparison with Eq. 15, consider another form that does not have the  $1/2$  power,

$$\Upsilon^*(\vec{f}_1, \vec{f}_2, \vec{f}_3, \vec{f}_4) = P(\vec{f}_1) \cdot P(\vec{f}_2) \cdot P(\vec{f}_3) \cdot P(\vec{f}_4) \quad (17)$$

Why is  $\Upsilon^*$  not the correct generalization of Boltzmann's *stosszahlansatz*? Although it does maintain symmetry between all the contacts, it cannot be correct because it implies that all four forces are statistically independent. They cannot be, because static equilibrium has removed two degrees of freedom. On the other hand, Eq. 15 does not imply statistical independence because the  $1/2$  power ruins normalization and therefore  $P^{1/2}(\vec{f})$  cannot be interpreted as a probability distribution. Furthermore, the removal of the two degrees of freedom through Newton's second law implies that the probability  $\Upsilon$  of four specific forces colliding in a grain should have units of (Newtons) $^{-2}$  rather than (Newtons) $^{-4}$  as we see in  $\Upsilon^*$ . The  $1/2$  power in Eq. 15 solves this problem, too.

In summary, we began this section with arguments that force correlations should not arise very strongly, if at all, through the closure of grain loops. This produced an expression  $\Upsilon$  that may be interpreted as the probability that a set of four specific contact forces may "collide" with one another in a stable grain. This result will enable the ergodicity proof for contact forces in the next section.

TABLE I: Phase space conventions.

Scale	Number of Grains	State Variable	Density of States
Grain	1	$g = (w_x, w_y, \theta_1, \dots, \theta_4)$	$\rho(g)$
Set of Grains	$m$	$\gamma = (g_1, g_2, \dots, g_m)$	$\rho(\gamma)$
Packing	$N$	$\Gamma = (g_1, g_2, \dots, g_N   \mathcal{C})$	$\rho(\Gamma)$

## IV. THE SELF-ERGODIC THEOREM

### A. The Granular Transport Equation

To simplify notation, Table I defines the conventions that describe the states of (1) single grains, (2) sets of grains, and (3) entire packings. The single-grain state variable  $g$  shown here assumes  $Z = 4$  for every grain. This may be easily generalized for grains with  $Z \neq 4$  but doing so adds no insight to the physics at this stage.

Using these conventions, we proceed to develop a granular contact force transport equation. Boltzmann wrote a transport equation to track the changes in the single particle distribution function  $f(\vec{v})$  through time. In writing the analogous equation for contact forces we must use changes through space, not time, because self-ergodicity operates across space. We will therefore perform a transport of forces similar to the transport contained in the  $q$  model, following successive cross-sectional layers of grains. We use the word "layer" as it was defined with Fig. 3, so that "translating" refers to the continuous motion of the cross-sectional line that picks out the set of grains in a layer. If the container is 2D, rectangular, and frictionless, then we will have two spatial axes along which to propagate layers of grains subject to the conservation laws. We cannot perform the transport in a diagonal direction because then the length of layers will not be constant and neither will the total perpendicular force contained within them. This transport in a finite container is the microcanonical version of the transport because the system is closed. Alternatively, we can perform the transport in an extremely large packing (perhaps infinite) and track only a finite cross sectional segment that propagates across the packing in any random spatial direction, not only in the  $x$  or  $y$  direction. In that case, the conservation law will not be exact because some force will be constantly entering and exiting the segment at both of its ends. However, the longer the segment of grains is, then the less significant those fluctuations become and the more closely it approximates an exact conservation law. This is the canonical version of the transport, because the segment is in contact with an infinite reservoir of forces at each end. It does not matter which way we imagine the transport to occur, nor in what direction. This will be re-addressed at the end.

Suppose Maxwell's demon chooses the layer of grains that we will use as our starting point. With malicious intent, he searches through the entire ensemble of packings and chooses a packing that has a single layer with a den-

sity of single grain states  $\rho_0(g)$  dissimilar to the density of its overall packing. That is,  $\rho_0(g) \neq \rho(g)$ . From this starting point, we wish to discover what happens to the density of layer states as a function of  $x$  as we propagate the cross sectional line in the  $x$  direction ( $x$  being perpendicular to the layer), and so we write  $\rho(g) = \rho(g, x)$ . As we translate from  $x \rightarrow x + \Delta x$  with  $\Delta x \lll D_{\text{particle}}$  (the grain diameter), a small fraction of the grains in the layer will no longer be intersected by the line and hence will exit the layer. Also, some new grains will be intersected by the cross-sectional line and hence they will join the layer. If the layer contains  $M$  grains, then the number of grains expected to leave the layer in  $\Delta x$  is  $m = M\Delta x/D_{\text{particle}}$ . If the fabric is constant across the packing (so that  $M$  is the same for every layer to good approximation), then this is also the number of grains expected to join the layer in  $\Delta x$ . For sufficiently small  $\Delta x$  the grains exiting the layer will be sufficiently far apart to be statistically independent. The probability for a particular set of  $m$  grains to leave during  $\Delta x$  is therefore

$$P_{\text{out}}(\gamma) = \prod_{\alpha=1}^m \rho_1(g_\alpha) \quad (18)$$

The probability for a particular set of  $m$  grains to enter during  $\Delta x$  can be written in terms of the generalized *stosszahlansatz* from Eq. 15, except that we must be careful because in general  $P(\vec{f})$  for contacts that are on one hemisphere of the grains will not be the same as for the other hemisphere. That is because  $\rho(g)$  is evolving layer-by-layer, and  $P = P[\rho]$ . Therefore, we write the *stosszahlansatz* in the form,

$$\Upsilon^\pm(g) = \prod_{\eta^+} \sqrt{P'(\vec{f}_\eta(g))} \prod_{\eta^-} \sqrt{P(\vec{f}_\eta(g))} \quad (19)$$

where  $\eta^-$  refers to all the contacts on grain  $\alpha$  in the reverse direction of the transport, and  $\eta^+$  refers to its contacts in the forward direction of the transport. Likewise,  $P$  represents the distribution of external forces in the reverse direction and  $P'$  the distribution of contacts in the forward direction.  $P'$  is not known because it looks forward one step beyond the present state in the transport process. This difficulty is due to the inherent nature of granular materials: every grain touches a network containing every other grain, so there is no way to treat the transport process as causal in one direction, only. Fortunately, we do not need to know the form of  $P'$  to obtain the ergodic proof. Because the grains entering the layer are statistically independent for sufficiently small  $\Delta x$ , we may write the probability for a particular set of  $m$  grains to enter during that interval as

$$P_{\text{in}}(\gamma') = \mathcal{N} \prod_{\alpha=1}^m \Upsilon^\pm(g'_\alpha) \quad (20)$$

where  $\mathcal{N}$  is for normalization.

Because every new layer must exactly obey the conservation law no matter how large or small  $\Delta x$ , we may

consider this “in-out” structure to be analogous to Boltzmann’s binary collisions, except that they are “m-nary” collisions and that each iteration  $\Delta x$  contains only one of them. The probability of having a particular collision  $\gamma \rightarrow \gamma'$  is

$$\begin{aligned} n(\gamma \rightarrow \gamma') &= \mathcal{N}(\gamma) \prod_{\alpha=1}^m \rho(g_\alpha) \prod_{\eta^+} \sqrt{P'(\vec{f}_\eta(g'_\alpha))} \\ &\quad \times \prod_{\eta^-} \sqrt{P(\vec{f}_\eta(g'_\alpha))} \\ &= \mathcal{N}(\gamma) \prod_{\alpha=1}^m \rho(g_\alpha) \Upsilon^\pm(g'_\alpha) \end{aligned} \quad (21)$$

where  $\mathcal{N}$  is for normalization. The number of times that  $\gamma$  will go to any set of single grain states is

$$n(\gamma \rightarrow \text{all}) = \int_{\odot} \mathcal{D}g'_1 \cdots \mathcal{D}g'_m \mathcal{N}(\gamma) \prod_{\alpha=1}^m \rho(g_\alpha) \Upsilon^\pm(g'_\alpha) \quad (22)$$

where the integrals are carried out only over the “stable” region  $\odot$  in  $g_i$ , that is, the region where none of the contact forces are tensile. Likewise,

$$n(\text{all} \rightarrow \gamma) = \int_{\odot} \mathcal{D}g'_1 \cdots \mathcal{D}g'_m \mathcal{N}(\gamma') \prod_{\alpha=1}^m \rho(g'_\alpha) \Upsilon^\pm(g_\alpha) \quad (23)$$

Because every layer must connect to another layer, we insist that

$$n(\gamma \rightarrow \text{all}) = \prod_{\alpha=1}^m \rho(g_\alpha) \quad (24)$$

and therefore

$$\mathcal{N}^{-1}(\gamma) = \int_{\odot} \mathcal{D}g'_1 \cdots \mathcal{D}g'_m \prod_{\alpha=1}^m \Upsilon^\pm(g'_\alpha) \quad (25)$$

so that

$$\mathcal{N}(\gamma) = \mathcal{N}[P, P'] = \mathcal{N}(\gamma') \quad (26)$$

which shall be important below.

To determine the rate of change in  $\rho(g)$  during the transport process, we write,

$$\frac{d}{dx} \rho(g_1) = \int_{\odot} \mathcal{D}g_2 \cdots \mathcal{D}g_m [n(\text{all} \rightarrow \gamma) - n(\gamma \rightarrow \text{all})] \quad (27)$$

## B. Counting States for Granular Packings

To evaluate how this transport equation behaves, we need a metric, similar to Boltzmann’s  $H$ , that will indicate how many packing states correspond to any particular  $\rho(g)$ . The “most entropic”  $\rho(g)$  is the one that



arises in the greatest number of packings. As explained in Ref. [12], the generalized *stosszahlansatz* enables the explicit counting of states as a functional of  $\rho(g)$ . First we discretize  $\rho(g) \rightarrow \nu_{ijklmn}$ , where the six arguments of  $g$  have been broken into small bins of size  $\Delta w$  and  $\Delta\theta$  and indexed as  $w_{xi}, w_{yj}, \theta_{1k}, \dots, \theta_{4n}$ . Each bin is further divided into  $S$  smaller bins to enable the typical binomial counting method for particles that do not have Pauli exclusion.  $S$  shall drop out of the equations in the continuum and thermodynamic limits when  $\Delta g = (\Delta w)^2(\Delta\theta)^4 \rightarrow 0$  as  $N \rightarrow \infty$ . For now, with  $S$  we may write the number of states corresponding to a particular  $\nu_{ijklmn}$ ,

$$\Omega\{\nu_{ijklmn}\} = \prod_i \prod_j \prod_k \prod_l \prod_m \prod_n \left[ \frac{(S-1+\nu_{i\dots n})!}{(S-1)! (\nu_{i\dots n})!} \right] \times \left( \sum_{i\dots n} \nu_{i\dots n} \right)! [\Upsilon_{i\dots n} \Psi_{i\dots n}]^{\nu_{i\dots n}} \quad (28)$$

Recall  $\Upsilon$  was derived in Eq. 15 from Newton's third law in Eq. 3 and is the fraction of grains at any locus in phase space that satisfy Newton's third law with their neighbors. Likewise  $\Psi$  was derived from the Newton's second law in Eq. 3. It evaluates to zero at a locus of phase space where any of the  $g_\alpha$  cannot be stable apart from tensile forces, and it evaluates to unity elsewhere. We will divide the range of  $g$ , call it  $\mathcal{G}$ -space, into the two regions

$$\int_{\mathcal{G}} \mathcal{D}g = \int_{\odot} \mathcal{D}g + \int_{\otimes} \mathcal{D}g \quad (29)$$

where  $\odot$  contains all the grain configurations that have compressive contact forces and  $\otimes$  contains all the grain configurations that have one or more tensile contact forces. Since we are dealing with cohesionless grains,  $\odot$  is the stable region and  $\otimes$  is the unstable region. For simplicity we will restrict all further mathematics to  $\odot$  so we may drop  $\Psi$  from the expressions.

We define  $H$  as

$$H \triangleq \lim_{\substack{N \rightarrow \infty \\ \Delta g \rightarrow 0}} \log \Omega \quad (30)$$

The natural logarithm of  $\Omega$ , using Sterling's approximation, may be written

$$\log \Omega = \sum_{i,j,k,l,m,n} [(S-1+\nu_{i\dots n}) \log(S-1+\nu_{i\dots n}) - (S-1) \log(S-1) - \nu_{i\dots n} \log \nu_{i\dots n} + \nu_{i\dots n} \log \Upsilon_{i\dots n}] \quad (31)$$

Expanding the first term in a Taylor series around  $\nu_{i\dots n} = 0$ , setting  $S = N\Delta g$ , and taking the continuum and thermodynamic limits such that  $S \gg \nu_{i\dots n}$ , we obtain

$$H = - \int_{\odot} \mathcal{D}g \rho(g) \log \frac{\rho(g)}{\Upsilon(g)} \quad (32)$$

The functional  $H = H[\rho(g)]$  is a measure of the number of states in  $\rho(\Gamma)$  that correspond to  $\rho(g)$ , and is in fact the generalization of Shannon's entropy for granular contact forces. We may note that the  $H$  functional may be written,

$$H = K - h \quad (33)$$

where

$$h = \int_{\odot} \mathcal{D}g \rho(g) \log \rho(g) \quad (34)$$

looks more like Boltzmann's original version of  $H$ , but where the correction term  $K$  accounts for the very constraining, intimate connectedness of the grains in a packing,

$$K = \int_{\odot} \mathcal{D}g \rho(g) \log \Upsilon(g) \quad (35)$$

Since  $\Upsilon < 1$ ,  $K < 0$  and we see that Newton's third law reduces the entropy of a granular packing as we would expect.

During a transport process,  $\rho(g)$  must be allowed to evolve layer-by-layer, and therefore so must  $P(\vec{f})$ . Hence, we distinguish between the hemispheres of a grain and use the form of  $\Upsilon$  from Eq. 19 to write,

$$H = - \int_{\odot} \mathcal{D}g \rho(g) \log \frac{\rho(g)}{\Upsilon^\pm(g)} \quad (36)$$

### C. Behavior of $\rho$ and $H$ in the Transport Process

With this metric in hand, the question we wish to address is whether  $(d/dx)H > 0$  during the transport process described above. Differentiating  $H$ ,

$$\frac{d}{dx} H = \int_{\odot} \mathcal{D}g \left\{ \frac{d}{dx} \rho(g) \left[ 1 + \log \frac{\Upsilon^\pm(g)}{\rho(g)} \right] + \rho(g) \frac{d}{dx} \log \Upsilon(g) \right\} \quad (37)$$

The last term (call it  $\chi$ ) may be expanded,

$$\begin{aligned} \chi &= \int_{\odot} \mathcal{D}g \rho(g) \frac{d}{dx} \log \Upsilon(g) \\ &= \int_{\odot} \mathcal{D}g \rho(g) \frac{d}{dx} \log \prod_{\eta} \sqrt{P(\vec{f}_{\eta}(g))} \\ &= \frac{1}{2} \sum_{\eta} \int_{\odot} \mathcal{D}g \rho(g) \frac{d}{dx} \log P(\vec{f}_{\eta}(g)) \end{aligned} \quad (38)$$

and then evaluated by changing the integration from a sum over all grains to a sum over all contacts,

$$\begin{aligned} \chi &= \int_0^\infty d\vec{f} P(\vec{f}) \frac{d}{dx} \log P(\vec{f}) \\ &= \frac{d}{dx} \int_0^\infty d\vec{f} P(\vec{f}) \\ &= 0 \end{aligned} \quad (39)$$

Substituting Eqs. 22, 23, and 27 into  $(d/dx)H$  and then factoring out  $\mathcal{N}$  as allowed by Eq. 26,

$$\begin{aligned} \frac{d}{dx}H &= \mathcal{N} \int_{\odot} \mathcal{D}g_1 \cdots \mathcal{D}g_m \int_{\odot} \mathcal{D}g'_1 \cdots \mathcal{D}g'_m \\ &\times \left( \prod_{\alpha} \rho(g'_\alpha) \Upsilon^{\pm}(g_\alpha) - \prod_{\alpha} \rho(g_\alpha) \Upsilon^{\pm}(g'_\alpha) \right) \\ &\times \left[ 1 + \log \frac{\Upsilon^{\pm}(g_1)}{\rho(g_1)} \right] \end{aligned} \quad (40)$$

Since we integrate over  $\odot$  for all  $g_\alpha$  and  $g'_\alpha$ , we may swap variables and average the various equivalent expressions to obtain,

$$\begin{aligned} \frac{d}{dx}H &= \frac{\mathcal{N}}{2m} \int_{\odot} \mathcal{D}g_1 \cdots \mathcal{D}g_m \int_{\odot} \mathcal{D}g'_1 \cdots \mathcal{D}g'_m \\ &\times \left( \prod_{\alpha} \rho(g'_\alpha) \Upsilon^{\pm}(g_\alpha) - \prod_{\alpha} \rho(g_\alpha) \Upsilon^{\pm}(g'_\alpha) \right) \\ &\times \log \frac{\prod_{\alpha} \rho(g'_\alpha) \Upsilon^{\pm}(g_\alpha)}{\prod_{\alpha} \rho(g_1) \Upsilon^{\pm}(g'_\alpha)} \end{aligned} \quad (41)$$

By inspection of the integrand we see that it is never negative for any part of the region of integration. Hence,

$$\frac{d}{dx}H \geq 0 \quad (42)$$

so that the entropy of the packing can only increase layer-by-layer. Furthermore,  $(d/dx)H = 0$  if and only if

$$\prod_{\alpha} \rho(g'_\alpha) \Upsilon^{\pm}(g_\alpha) = \prod_{\alpha} \rho(g_\alpha) \Upsilon^{\pm}(g'_\alpha) \quad \forall \quad g_\alpha, g'_\alpha \quad (43)$$

and this is true if and only  $(d/dx)\rho(g) = 0$  for all  $g$ . When that is the case, then  $P = P'$ .

We can draw the following conclusions, which depend upon large  $M$  and the assumption that the generalized *stosszahlansatz* is valid. First, if there exists a layer in a granular packing that is not at maximum entropy, then the surrounding layers in both directions will (essentially always) relax to maximum entropy. However, beginning from any layer that is already relaxed at maximum entropy, then it is highly unlikely that its neighbors will fluctuate very far away from maximum entropy. Hence, the existence of any layer far from maximum entropy is exceedingly unlikely and such layers will practically never be found. Therefore, essentially all granular packings *must* exist at maximum entropy. The propagation of contact forces in a granular material is *truly* ergodic in the special form that we are calling self-ergodic.

This also proves that Edward's flat measure in the geometry of packings is not what determines the flat measure in the contact forces. Suppose (for the sake of illustration) that Edwards' flat measure were not correct such that some stable  $\Gamma$  states were more probable than others. The self-ergodicity theorem has proven that  $\rho(g)$  for those more probable  $\Gamma$  states must be identical to

the  $\rho(g)$  for the less probable  $\Gamma$  states, as long as the *stosszahlansatz* is valid. Therefore, each packing will have the same ergodicity of contact forces regardless of its relative probability in  $\Gamma$  space.

We may compare this to the Poincaré Theorem, which tells us that there is a Gibbsian flat measure over the entire Poincaré cycle (to within arbitrarily small distances from every state). Whether there is or not such a Gibbsian flat measure in thermodynamics is unimportant to Boltzmann's proof. That proof tells us that any non-Maxwellian portion of the Poincaré cycle is non-Maxwellian precisely because the *stosszahlansatz* was pathologically violated in the segment leading up to it. Because we know the *stosszahlansatz* is violated only rarely, not greatly, and not for long, this proves that essentially every part of the Poincaré cycle has the Maxwell-Boltzmann distribution of velocities, whether or not the cycle itself has a flat measure. Thus, the dominance of the Maxwell-Boltzmann distribution is proven independently of Gibbsian flatness. Boltzmann's practical ergodicity does not depend upon ultimate mathematical ergodicity. For exactly the same reason, the proof of self-ergodicity for granular contact forces and the derivation of  $\rho(g)$  are independent of Edwards' flat measure.

However, this analogy is not exactly correct. Boltzmann's practical ergodicity tells us that every tiny segment of the Poincaré cycle is dominated by the Maxwellian distribution, so that only a tiny amount of dynamics are needed to leave any non-Maxwellian state and settle into maximum entropy. So both the Poincaré ergodicity and the Boltzmann ergodicity are attained by traveling along the trajectory in phase space. Static granular packings, on the other hand, do not travel along any trajectory in phase space. The self-ergodicity proven above depends upon contact forces maintaining static spatial relationships, not travelling and interacting through spatio-temporal ones. Thus, the self-ergodicity theorem does not depend upon any travelling through  $\Gamma$  space at all. Boltzmann's proof obviated the need to travel the entire Poincaré cycle and showed that the system need travel only a tiny segment of it. The self-ergodicity theorem on the other hand says that a granular packing need not travel through  $\Gamma$  space at all, because it has special relationships between its own subspaces built into its single locus in  $\Gamma$  space. This differentiates self-ergodicity from the ordinary ergodicity of thermodynamics.

#### D. Derivation of the Density of States and $P(f)$

The self-ergodicity theorem tells us that  $(d/dx)H = 0$  is the state of essentially every possible layer in every static granular packing and that the sufficient and necessary condition for this state is given by Eq. 43. This can



be written in the form,

$$\prod_{\alpha=1}^m \frac{\rho(g_\alpha)}{\Upsilon^\pm(g_\alpha)} = \prod_{\alpha=1}^m \frac{\rho(g'_\alpha)}{\Upsilon^\pm(g'_\alpha)} \quad \forall g_\alpha, g'_\alpha \quad (44)$$

which implies that either side of the equation may be written as equal to a constant. Taking the logarithm,

$$\sum_{\alpha=1}^m \log \frac{\rho(g_\alpha)}{\Upsilon^\pm(g_\alpha)} = C \quad (45)$$

and we see that is in the form of a conservation law. Its most general solution is when  $C$  is written as a linear combination of all conserved quantities. Since we did not specify the orientation of the layer or the direction of transport, this result is valid for all orientations and directions. Therefore, all components of the duress tensor from Eq. 4 must be conserved.

Is fabric conserved in the transport process? By obvious geometry, each grain has a contact angle in the opposite direction of the corresponding contact in the adjacent layer. Thus, the distribution of contact angles in one layer  $P_\theta(\theta)$  must be related to the distribution in the adjacent layer  $P'_\theta(\theta)$  by

$$R_\pi(P_\theta) = P'_\theta \quad (46)$$

where  $R_\pi$  is the operator for  $\pi$ -radian rotations. However, it is not necessarily true that  $R_\pi(P_{4\theta}) = P'_{4\theta}$ . Thus, we cannot say *a priori* that

$$R_\pi(\rho(g)) = \rho'(g) \quad (47)$$

However, we can make another assumption additional to the *stosszahlansatz*. We assume that the construction method of the packing was such that the ensemble has  $R_\pi$  symmetry. Construction methods such as compacting, shearing, and shaking should satisfy that requirement. Pouring in gravity does not. With this added assumption,  $(d/dx)\rho(g) = 0$  implies that

$$R_\pi(P_{4\theta}) = P_{4\theta} \quad (48)$$

and

$$P_{4\theta} = P'_{4\theta} \quad (49)$$

so that fabric is conserved in the transport process. Therefore, the conserved quantities in the transport process are the same as the last two delta functions at the end of Eq. 3.

Writing Eq. 45 in terms of the conserved quantities, we obtain for every  $g_\alpha \in \odot$

$$\log \frac{\rho(g_\alpha)}{\Upsilon(g_\alpha)} = \beta_x w_x^\alpha + \beta_y w_y^\alpha + \mu(\theta_1, \dots, \theta_4) \quad (50)$$

and solving for  $\rho$ ,

$$\rho(g) = G(\theta_1, \dots, \theta_4) \Psi(g) \Upsilon(g) e^{-\beta_x w_x - \beta_y w_y} \quad (51)$$

(Recall that  $\Psi$  is the function that enforces the bounds on  $\odot$ , evaluating either to unity or zero if the cohesionless grain is stable or unstable, respectively.)  $G(\theta_1, \dots, \theta_4)$  is the fabric partition factor. Eq. 51 is identical to the equation derived in [12] by counting states and assuming maximum  $\log \Omega$ , using Lagrange multipliers to conserve fabric and stress. Remembering that  $\Upsilon$  is a functional of  $P(\vec{f})$  and that

$$P(\vec{f}) = \int_{\odot} \mathcal{D}g \quad \rho(g) \delta^2(\vec{f} - \vec{f}(g)) \quad (52)$$

we see that Eq. 51 and 52 form a recursion so that  $\rho$  may be solved numerically when stress and fabric are specified. Solving for  $\rho(g)$  provides everything that can be known about the density of single grain states, including  $P(f)$ .

## V. EMPIRICAL VALIDATION OF SELF-ERGODICITY

The qualitative arguments of Sec. III told us that we could discard any force correlation possibly arising through force loops. This generalized *stosszahlansatz* must now be tested to show that any discarded correlations were truly inessential. We perform this test by solving for  $\rho(g)$  and comparing the results to numerical simulations of granular packings.

For the present Eq. 51 has been solved in the isotropic case, assuming  $Z = 4$  for every grain with the approximation

$$\rho_g(w_x, w_y, \theta_\beta) \approx \rho_w(w_x, w_y) \rho_\theta(\theta_\beta) \Psi(w_x, w_y, \theta_\beta) \quad (53)$$

as described in [12]. This modified separability assumes no correlation between the loads and fabric apart from the truncating effect of  $\Theta_S$ . The physical idea is that correlation does arise predominantly because nature disallows unstable grains. Empirical results have shown this to be correct [12]. In the remainder of this paper, “the theory” refers to the resulting numerical solution.

The predictions of the theory have been overwhelmingly validated. A subset of these results have been reported earlier [18]. Fig. 12 shows  $P_f(f)$  obtained from the theory and from the DEM data including all grains having  $Z > 2$ . The agreement is even better when only the  $Z = 4$  grains from the DEM are included, as shown in Fig. 13. It should be noted that there are no free parameters in the theory that could be adjusted to obtain these good fits. The predictions either fit the empirics or they do not. As it turns out, they are in such remarkable agreement that we may claim that the theory’s prediction is proven correct.

Fig. 14 shows  $P_x(f_x)$  obtained from the theory and from the DEM data including all grains having  $Z > 2$ . Fig. 15 shows the comparison for the  $Z = 4$  population of the DEM. Again, the prediction has been proven correct.

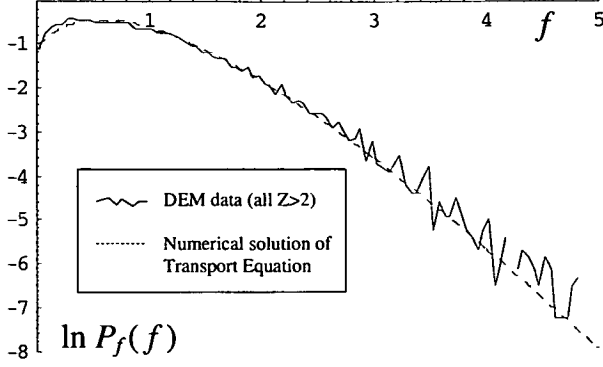


FIG. 12: Semi logarithmic  $P_f(f)$  obtained in numerical solution of the transport equation and from DEM data, all  $Z > 2$ .

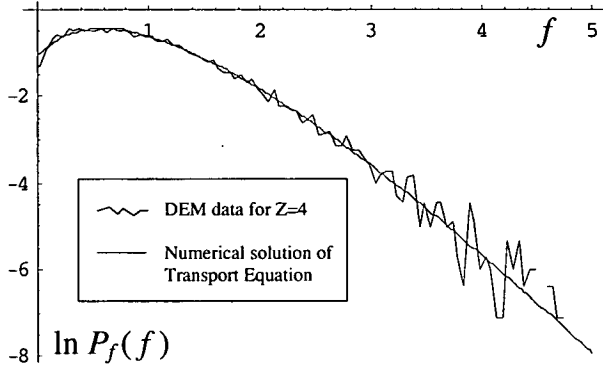


FIG. 13: Semi logarithmic  $P_f(f)$  obtained in numerical solution of the transport equation and from  $Z = 4$  population of DEM.

It should also be noted that the forms for  $P_{\theta,f}(f,\theta)$  and  $P_x(f_x)$  are conjugate to one another in that it is possible to convert back and forth between them using Youngquist's transform (when  $P_x(f_x)$  is known for all arbitrary rotations of the Cartesian axes, which for the isotropic case is trivial) [19]. Functional forms have been fitted to the empirical data for  $P_f(f)$  and  $P_x(f_x)$  from these simulations, and applying Youngquist's transform does produce the correct functional forms to fit their conjugate distributions. This transform proves analytically that when  $P_f(f)$  has an exponentially decaying form, then  $P_x(f_x)$  is a series sum of modified Bessel functions of the second kind. The two knees indicative of that type of Bessel function are clearly visible in Figs. 14 and 15.

The shear ratio  $s = (w_x - w_y)/(w_x + w_y)$  and the grain pressure  $t = w_x + w_y$ , calculated for each grain, are predicted by the theory to be statistically independent (unlike  $w_x$  and  $w_y$ ). The data from the DEM have been sorted into separate populations by  $Z$  so that,

$$P_{st}(s,t) = \sum_{Z=3}^5 n_Z P_{st}^{(Z)}(s,t) \quad (54)$$

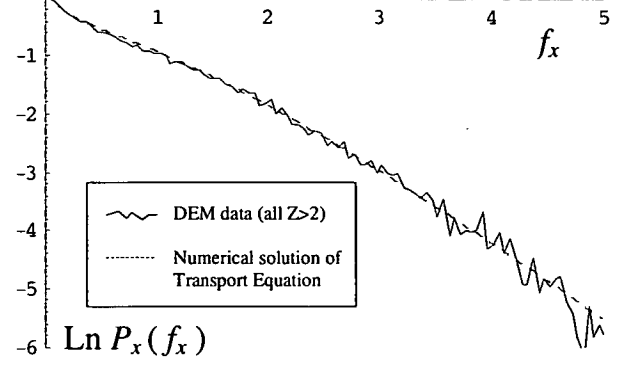


FIG. 14: Semi logarithmic  $P_x(f_x)$  obtained in numerical solution of the transport equation and from DEM data, all  $Z > 2$ .

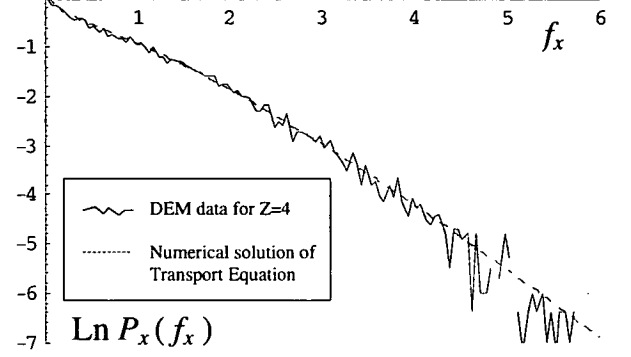


FIG. 15: Semi logarithmic  $P_x(f_x)$  obtained in numerical solution of the transport equation and from  $Z = 4$  population of DEM data.

where  $n_Z$  is the fraction of grains within each  $Z$  population and  $P_{st}^{(Z)}(s,t)$  is the distribution of each population taken separately. Then, we find that the  $s$  and  $t$  parameters are indeed statistically independent within each population considered separately,

$$P_{st}^{(Z)}(s,t) = P_s^{(Z)}(s) P_t^{(Z)}(t) \quad (55)$$

for each value of  $Z$ . Again, the predictions of the theory have been validated.

Fig. 16 compares the theory's prediction and the DEM data for the distribution of the shear ratio  $P_s(s)$ . The agreement is quite good, even without sorting by  $Z$ . Since the theory assumed  $Z = 4$  we wish to test whether the other  $Z$  populations fit the same form. For comparison we use the functional form that was fitted to the theory's solution,

$$P_s(s) = \cos(\pi s/2) e^{-8s^2}. \quad (56)$$

Remarkably, we find that the same form fits all three populations reasonably well after we write the standard deviation as

$$\sigma = 1/Z \quad (57)$$

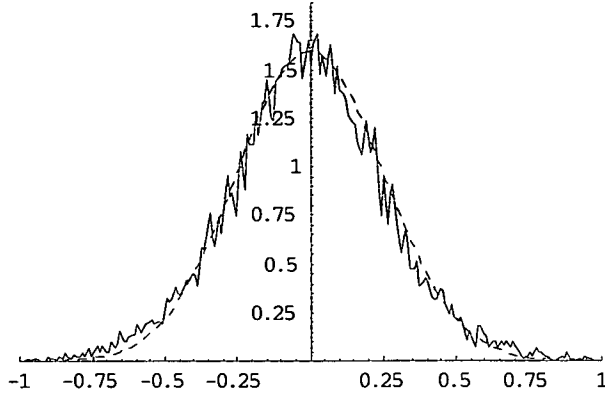


FIG. 16:  $P_s(s)$  obtained in numerical solution of the transport equation and from DEM data including all grains having  $Z > 2$ .

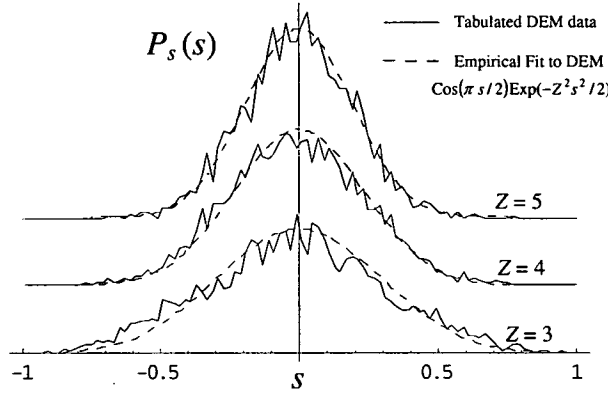


FIG. 17:  $P_s(s)$  in DEM data segregated by  $Z$ .

This form compared to all three  $Z$  populations is shown in Fig. 17.

Examining the distribution of grain pressures,  $P_t(t)$  where  $t = w_x + w_y$ , Fig. 18 compares the  $Z = 4$  population of the DEM with the theory's prediction. Fig. 19 makes the same comparison semi logarithmically. These demonstrate good agreement. However, the DEM data with all  $Z$  populations included does not match the theory's predictions very well due to the presence of the  $Z = 3$  and  $Z = 5$  grains. Nevertheless, as was done for  $P_s(s)$ , an interesting comparison can be made between all these populations by finding a functional fit and parameterizing it in terms of  $Z$ . A function that fits the theory's prediction reasonably well over the region of experimental interest ( $0 \leq t \lesssim 3$ ), is

$$P_t(t) = t^{\beta-1} e^{-\beta t} \quad (58)$$

with  $\beta = 5$ . After segregating the DEM data by  $Z$  we find that all three populations do fit this same form as shown in Figs. 20 and 21, but using  $\beta = 2Z - 4$ .

This provides empirical proof that the generalized *stosszahlansatz* does not throw away any of the corre-

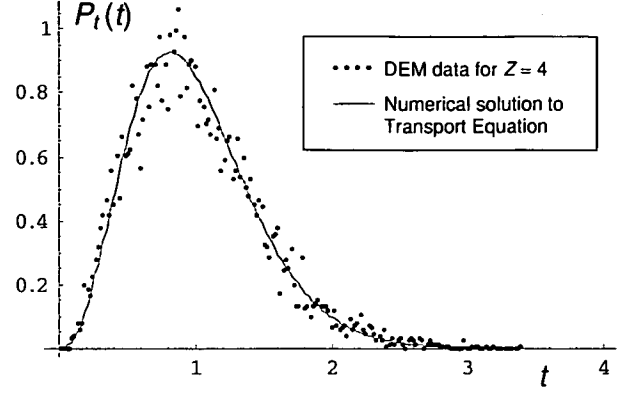


FIG. 18:  $P_t(t)$  obtained from numerical solution of the transport equation and from DEM data including only grains having  $Z = 4$ .

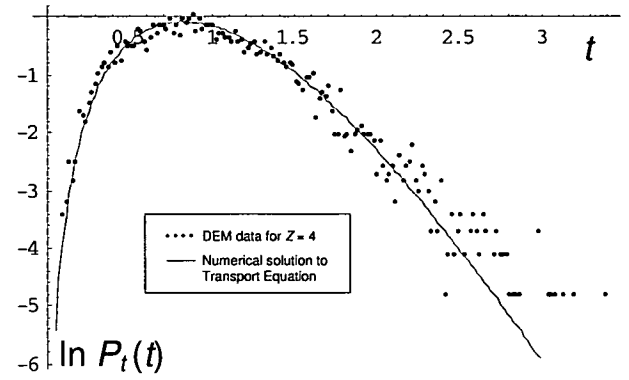


FIG. 19: Semi logarithmic comparison of  $P_t(t)$  obtained from numerical solution of the transport equation and from DEM data including only grains having  $Z = 4$ .

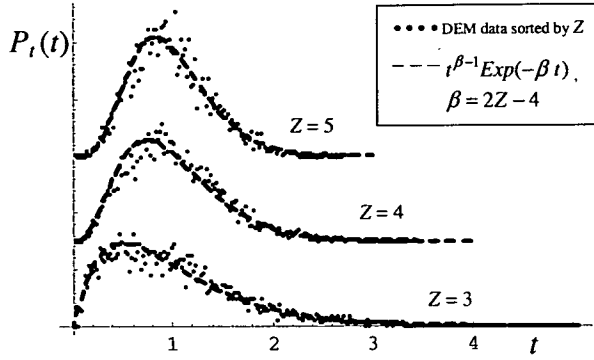
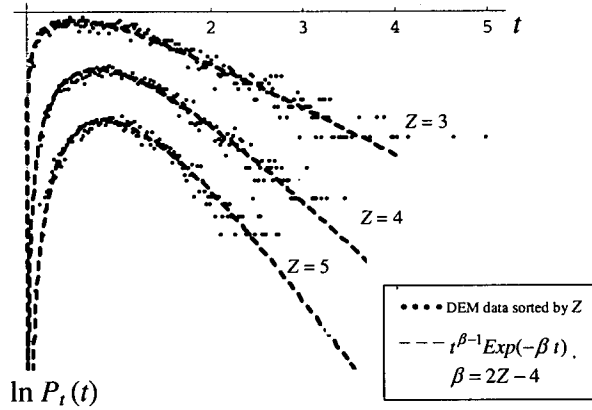
lations responsible for the major features of  $\rho_g$ , just like Boltzmann's original version does not throw away the essential features of the density of single particle states for the molecules in a dilute, thermalized gas.

## VI. SUMMARY AND CONCLUSIONS

This paper has proven that the propagation of granular contact forces is a truly ergodic process, although the nature of that ergodicity is more complex and interesting than what we find in thermal systems and so the term "self-ergodicity" appears to be a more appropriate description. On the way to making this proof, it generalized Boltzmann's *stosszahlansatz* and Shannon's entropy for granular contact forces. As a consequence of the proof, it found a second way to derive  $\rho(g)$ , obtaining agreement with the earlier method developed by the author. This  $\rho(g)$  is in outstanding agreement with empirical observations.

Because the percolation of forces is self-ergodic, essen-



FIG. 20:  $P_t(t)$  in the DEM, segregated by  $Z$ .FIG. 21: Semi logarithmic  $P_t(t)$  in the DEM, segregated by  $Z$ .

tially every granular packing of the class considered in this paper will exist in a state of maximum entropy, without first having to explore phase space at all. There are of course many significant classes of granular packings that will not be relaxed to maximum entropy, but these

have not been discussed here. They would include granular packings that were prepared to have abrupt changes in fabric somewhere within their bulk so that the density of states cannot be in its most relaxed state within the narrow band of grains on both sides of the interface. Another case would be the thin layer of grains at the top surface of a packing in gravity, where the self-weight introduces non-negligible stress gradients. However, solution of the more symmetric case considered here opens the door to solving more complex problems.

While this paper has addressed frictionless, isostatic packings exclusively, early tests of frictional packings demonstrate that the theory will apply surprisingly well there as well, with only minor modifications to include the effects of the frictional forces. It also appears easy to modify the theory to variable coordination number [13, 18]. In brief, the theory appears to be rigorous and widely applicable and should form the basis to solve a wide array of problems in granular statistical mechanics.

One statistical mechanics application in particular was first suggested by the author several years ago [20]. The idea is that, since granular contact force propagation is truly ergodic, then it is possible to define a contact force “temperature” and even a coordination number “chemical potential” to explain the partition of stress and fabric fluctuations throughout a granular packing, and possibly leading to a full theory of rheology. These observations were apparent when numerical solutions to the theory first proved robust and convergent, even before this formal proof of ergodicity was accomplished. That is because the numerical convergence discussed in the earlier publications was in fact an empirical proof of ergodicity, just as valid as the formal proof found in this paper. Once ergodicity is known, and once its characteristics are understood, then the temperature and chemical potential concepts fall out rather straightforwardly. A future publication will be forthcoming to fully explain these concepts along with a series of discrete element modeling simulations that have been performed to test them and to draw further conclusions.

[1] F. Radjai, M. Jean, J.-J. Moreau, and S. Roux, *Phys. Rev. Lett.* **77**, 274 (1996); C. Thornton, *Kona* **15**, 81 (1997); D.M. Mueth, H.M. Jaeger, and S.R. Nagel, *Phys. Rev. E* **57**, 3164 (1998); F. Radjai, S. Roux, and J.-J. Moreau, *Chaos* **9**, 544 (1999); S.J. Antony, *Phys. Rev. E* **63**, 011302 (2001); D.L. Blair, N.W. Mueggenburg, A.H. Marshall, H.M. Jaeger, and S. R. Nagel, *Phys. Rev. E* **63**, 041304 (2001); C.S. O’Hern, S.A. Langer, A.J. Liu, and S.R. Nagel, *Phys. Rev. Lett.* **86**, 111 (2001); J.M. Erikson, N.W. Mueggenburg, H.M. Jaeger, and S.R. Nagel, *Phys. Rev. E* **66**, 040301(R) (2002); C.S. O’Hern, S.A. Langer, A.J. Liu, and S.R. Nagel, *Phys. Rev. Lett.* **88**, 075507 (2002); J. Brujić, S.F. Edwards, D.V. Grinev, I. Hopkinson, D. Brujić, and H.A. Makse, *Faraday Disc.* **123**,

207 (2002); J.W. Landry, G.S. Grest, L.E. Silbert, and S.J. Plimpton, *Phys. Rev. E* **67**, 041303 (2003); J.H. Snoeijer, M. van Hecke, E. Somfai, and W. van Saarloos, *Phys. Rev. E* **67**, 030302(R) (2003); J.H. Snoeijer, M. van Hecke, E. Somfai, and W. van Saarloos, *Phys. Rev. E* **70**, 011301 (2004); J.H. Snoeijer, T.J.H. Vlugt, M. van Hecke, and W. van Saarloos, *Phys. Rev. Lett.* **92**, 054302 (2004); P.T. Metzger, *Phys. Rev. E* **69**, 053301 (2004).

[2] L.E. Silbert, G.S. Grest, and J.W. Landry, *Phys. Rev. E* **66**, 061303 (2002).

[3] Much of the discussion about whether the tail on a semi-logarithmic plot is flat (exponential) versus curved downward (decaying faster than exponential) would be resolved or moot if we agree to discuss only the *asymptotic*

- behavior of the tail. Undoubtedly the tail is curved downward for all finite  $f$ . The only issue is whether that curvature vanishes in the limit  $f \rightarrow \infty$ , which has important theoretical implications as discussed in the introduction of this paper. Even the Planck spectrum is curved downward for all finite energies, and does not display its true exponential character except in the limit  $E \rightarrow \infty$ . This question in relation to  $P_f(f)$  cannot be resolved using empirical data from finite packings, which contain only finite quantities of forces and hence cannot sustain a flat tail to infinity regardless of the fundamental statistical mechanics. What we can say, at least, is that the empirical data are consistent with the tail being asymptotically exponential, and that theoretical considerations such as in this paper imply that it truly is.
- [4] S.N. Coppersmith, C.-h. Liu, S. Majumdar, O. Narayan, and T.A. Witten, Phys. Rev. E **53**, 4673 (1996); C.-h. Liu, S.R. Nagel, D.A. Schecter, S.N. Coppersmith, S. Majumdar, O. Narayan, and T.A. Witten, Science **269**, 513 (1995).
  - [5] S.F. Edwards and R.B.S. Oakeshott, Physica A **157**, 1080 (1989).
  - [6] A. Mehta and S.F. Edwards, Physica A **157**, 1091 (1989); S.F. Edwards and C.C. Mounfield, Physica A **226**, 1 (1996); S.F. Edwards and D.V. Grinev, Chaos **9**, 551 (1999); S.F. Edwards and D.V. Grinev, Physica A **263**, 545 (1999); P.G. de Gennes, Rev. Mod. Phys. **71** S374 (1999); R.C. Ball and D.V. Grinev, Physica A **292**, 167 (2001); S.F. Edwards and D.V. Grinev, Physica A **294**, 57 (2001); A. Coniglio and M. Nicodemi, Physica A **296**, 451 (2001); S.F. Edwards and D.V. Grinev, Physica A **302**, 162 (2001); V. Colizza, A. Barrat, and V. Loreto, Phys. Rev. E **65**, 050301(R) (2002); A. Fierro, M. Nicodemi, and A. Coniglio, Phys. Rev. E **66**, 061301 (2002); R. Blumenfeld and S.F. Edwards, Phys. Rev. Lett. **90**, 114303 (2003); A. Coniglio, A. Fierro, and M. Nicodemi, cond-mat/0305175 (unpublished).
  - [7] M.L. Nguyen and S.N. Coppersmith, Phys. Rev. E **59**, 5870 (1999).
  - [8] M.E. Cates, J.P. Wittmer, J.-P. Bouchaud, and P. Claudin, Phys. Rev. Lett. **81**, 1841 (1998).
  - [9] C. Eloy and E. Clément, J. Phys. I (France) **7**, 1541 (1997); O. Narayan, Phys. Rev. E **63**, 010301(R) (2000).
  - [10] J.H. Snoeijer, T.J.H. Vlugt, W.G. Ellenbroek, M. van Hecke, and J.M.J. van Leeuwen, Phys. Rev. E **70**, 061306 (2004).
  - [11] B.P. Tighe, J.E.S. Socolar, D.G. Schaeffer, W.G. Mitchener, and M.L. Huber, Phys. Rev. E **TBD**, TBD (TBD).
  - [12] P.T. Metzger, Phys. Rev. E **70**, 051303 (2004).
  - [13] P.T. Metzger, "Deriving the Density of States for Granular Contact Forces," Ph.D. Thesis (2005).
  - [14] The rationale for this density of states is provided in Ref. [12], but it is written in a more general form here.
  - [15] S.F. Edwards, Physica A **249**, 226 (1998); S.F. Edwards and D.V. Grinev, Physica A **302**, 162 (2001).
  - [16] A.V. Tkachenko and T.A. Witten, Phys. Rev. E **60**, 687 (1999); L.E. Silbert, D. Ertas, G.S. Grest, T.C. Halsey, and D. Levine, Phys. Rev. E **65**, 031304 (2002); A. Kasa-hara and H. Nakanishi, cond-mat/0312598 (2003).
  - [17] H. Troadec, F. Radjai, S. Roux, and J.C. Charmet, Phys. Rev. E **66**, 041305 (2002).
  - [18] P.T. Metzger and C.M. Donahue, Phys. Rev. Lett. **94**, 148001 (2005).
  - [19] R.C. Youngquist, P.T. Metzger, and K.N. Kilts, SIAM J. App. Math. **65**, 1855-69 (2005).
  - [20] P.T. Metzger, cond-mat/0403034v1 (March 2004).